



Published in final edited form as:

Free Radic Biol Med. 2016 June ; 95: 74–81. doi:10.1016/j.freeradbiomed.2016.03.012.

Broad-spectrum antimicrobial photocatalysis mediated by titanium dioxide and UVA is potentiated by addition of bromide ion via formation of hypobromite

Ximing Wu^{1,2,3,*}, Ying-Ying Huang^{2,3,*}, Yu Kushida^{2,4}, Brijesh Bhayana^{2,3}, and Michael R. Hamblin^{2,3,5,*}

¹Department of Emergency, First Affiliated College & Hospital, Guangxi Medical University, Nanning 530021, China

²Wellman Center for Photomedicine, Massachusetts General Hospital, Boston, MA 02114, USA

³Department of Dermatology, Harvard Medical School, Boston, MA 02115, USA

⁴Graduate School of Pharmaceutical Science, University of Tokyo, Japan

⁵Harvard–MIT Division of Health Sciences and Technology, Cambridge, MA 02139, USA

Abstract

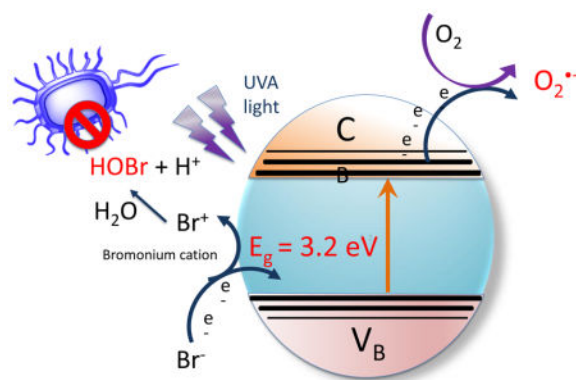
Antimicrobial photocatalysis involves the UVA excitation of titanium dioxide (TiO₂) nanoparticles (particularly the anatase form) to produce reactive oxygen species (ROS) that kill microbial cells. For the first time we report that the addition of sodium bromide to photoactivated TiO₂ (P25) potentiates the killing of Gram-positive, Gram-negative bacteria and fungi by up to three logs. The potentiation increased with increasing bromide concentration in the range of 0–10 mM. The mechanism of potentiation is probably due to generation of both short and long-lived oxidized bromine species including hypobromite as shown by the following observations. There is some antimicrobial activity remaining in solution after switching off the light, that lasts for 30 min but not 2 hours, and oxidizes 3,3',5,5'-tetramethylbenzidine. N-acetyl tyrosine ethyl ester was brominated in a light dose-dependent manner, however no bromine or tribromide ion could be detected by spectrophotometry or LC-MS. The mechanism appears to have elements in common with the antimicrobial system (myeloperoxidase + hydrogen peroxide + bromide).

Graphical abstract

*correspondence : hamblin@helix.mgh.harvard.edu.

*the first two authors made equal contributions

Publisher's Disclaimer: This is a PDF file of an unedited manuscript that has been accepted for publication. As a service to our customers we are providing this early version of the manuscript. The manuscript will undergo copyediting, typesetting, and review of the resulting proof before it is published in its final citable form. Please note that during the production process errors may be discovered which could affect the content, and all legal disclaimers that apply to the journal pertain.



Keywords

Antimicrobial photocatalysis; bacteria; titanium dioxide; sodium bromide; ultraviolet A; reactive oxygen species; hypobromite

Introduction

Photocatalysis is a rapidly growing technology that is being investigated for applications in solar energy conversion [1], and for environmental remediation and disinfection [2, 3]. Antimicrobial photocatalysis describes a process in which semiconductor nanoparticles such as titanium dioxide (TiO₂) are irradiated with UVA light to generate reactive oxygen species (ROS) in order to kill various types of microorganisms [4–8]. The procedure of antimicrobial photocatalysis has most often been suggested to be used in water purification [9], but other applications in medical science (orthopedics [10], dentistry [11] and surgery [12]) have also been proposed. Photoactivated TiO₂ is also beginning to be studied as a possible photodynamic treatment for cancer [13], and could also be used for precise sub-cellular inactivation at a molecular level [14]. The energy needed to excite an electron from the valence band to the conduction band in TiO₂ is 3.35 eV, which is equivalent to the energy of a photon with a wavelength of 360 nm. The released electrons in the conduction band can reduce oxygen to superoxide anion, while the positive holes left in the valence band can capture electrons from water, and oxidize water to hydroxyl radicals [15]. Hydrogen peroxide [16] and singlet oxygen [17] are also produced during photocatalysis. Together these oxidants can damage many biomolecules, and efficiently kill all the different classes of microorganisms, such as Gram-positive and Gram-negative bacteria, fungi, viruses and parasites, etc [18].

The advantages of antimicrobial photocatalysis (as compared to other kinds of photodynamic inactivation) are that: (1) it is a heterogeneous system so the solid TiO₂ could be removed from the reaction after use; (2) the TiO₂ is not easily photobleached in the same way that organic photosensitizers are photobleached by light delivery; and (3) TiO₂ can be activated by UVA wavelengths present in natural sunlight making the process suitable for remediation of contaminated wastes in outdoor settings. However there is still a lot of room to improve the efficiency of TiO₂ antimicrobial catalysis. Researchers are attempting to dope the TiO₂ with platinum or nitrogen or other materials in order to shift the activation

wavelength way from the UV to the visible range [19], and to fabricate different types of titania nanostructures such as TiO₂ nanotubes [20]. Our approach is to potentiate antimicrobial photocatalysis by the addition of simple non-toxic inorganic salts. In the present study we used P25 TiO₂ nanoparticles for our studies as they were commercially available and have been reported to be efficient at mediating photocatalysis. P25 has been reported to be composed of about 75% of the anatase crystalline isoform [21].

We recently discovered that antimicrobial photodynamic inactivation mediated by the phenothiazinium dye, methylene blue [22], and also by cationic functionalized fullerenes [23, 24] could be significantly potentiated by addition of the non-toxic salt, potassium iodide. We then went on to show that antimicrobial TiO₂ photocatalysis could be potentiated by addition of iodide anion (manuscript in preparation). We now report for the first time that antimicrobial TiO₂ photocatalysis can be significantly potentiated by addition of the non-toxic salt, sodium bromide.

Materials and methods

Chemicals

Titanium(IV) oxide (TiO₂) anatase P25, sodium bromide (NaBr), myeloperoxidase from human leukocytes (MPO), 3,3',5,5'-tetramethylbenzidine (TMB), 30% hydrogen peroxide (H₂O₂), and all other reagents were purchased from Sigma-Aldrich (St. Louis, MO) unless otherwise indicated. Hydroxyphenyl fluorescein (HPF) and Singlet Oxygen Sensor Green (SOSG) were purchased from (Molecular Probes, Invitrogen, Bedford, MA). TiO₂ and NaBr stock solutions were prepared in distilled H₂O (dH₂O) prior to use. We have presented the concentration of TiO₂ as mM (10mM = 800 µg/mL) to allow comparison with NaBr although the material is actually nanoparticles. We used two different buffers that were composed of 50 mM sodium phosphate at pH 7.4 and pH 5.5. All the photocatalysis experiments were carried out in 24-well plate under magnetic stirring except ROS-specific probe experiments.

Light source

We used a 360 nm UVA light-emitting diode (LED) light source (Larson Electronics LLC, Kemp, TX). The emission spectrum is shown in supplementary figure S1. The irradiance for all experiments was fixed at 16 mW/cm² (1 J/cm² delivered in 1 min), measured by a model IL-1700 research radiometer-photometer (International Light, Inc., Newburyport, MA). The emission spectrum was measured by a spectroradiometer (SPR-01; Luzchem Research, Inc., Ottawa, ON, Canada) and showed a peak emission at 365±5 nm.

Fluorescence probe assay for generation of specific reactive oxygen species (ROS)

96-well clear-bottom black plates were used for fluorescence probe experiments. SOSG or HPF (final concentration of 5 µM) was added to 10 mM TiO₂ with and without addition of 10 mM NaBr in a final volume of 200 µL PBS per well. The fluorescence was detected after each aliquot of 0.5–1 J/cm² (dose of light), using a fluorescence spectrometer (SpectraMax M5 plate reader, Molecular Devices, Sunnyvale, CA) The excitation and emission settings were used as recommended by the manufacturer of the probes: excitation 504 nm and

emission 525 nm for SOSG and excitation 490 nm and emission 515 nm for HPF, respectively.

3,3',5,5'-Tetramethylbenzidine (TMB) test for hypobromite

Stock solutions of TMB were prepared in DMSO at 1 mg/ml and kept at -20°C . Working solutions of TMB were freshly prepared by diluting 1 mL of stock solution in 9 mL 50 mM sodium acetate buffer, pH 5.5. A suspension of 10mM TiO_2 containing 10mM NaBr was exposed with stirring to different fluences of UVA light (0, 5, 10 and 40 J/cm^2) and after each fluence a 50 μL aliquot was withdrawn and added into 1 mL 0.1mg/ml TMB solution. After 180 minutes incubation time, 200 μL of the TMB reaction mixture was transferred to 96-well plate and absorbance at 655 nm was measured using a spectrometer (SpectraMax M5 plate reader, Molecular Devices, Sunnyvale, CA).

Bromination of N-acetyl tyrosine ethyl ester

Sample solutions (total volume 400 μL) contained TiO_2 (10mM), KI (100mM) and N-acetyl-L-tyrosine ethyl ester (10 mM) in PB buffer (pH 7.4, containing 10% methanol) were irradiated by UVA LED light (360nm) with magnetic stirring. An aliquot of solution (50 μL) was removed at different time point (30mins, 60mins, 120mins and 240 mins) and centrifuged at 4000 rpm. The supernatants were collected for the LCMS analysis. The LCMS analyses were performed on an Agilent 1260 LC system equipped with a triple-quad mass spectrometer. The LC conditions were: column: C18, 2.1×50 mm, 1.8 μm ; elution gradient: solution A = acetonitrile, solution B = 10 mM ammonium acetate in water, 2% \rightarrow 100% of A over 6 min with a flow rate of 0.2 mL/min; ionization mode: negative; injection volume: 5 μL .

Tribromide generation assays

In order to detect any production of bromine we attempted to detect the presence of tribromide ion (Br_3^-) which is quantitatively formed from the reaction between Br_2 and Br^- [25]. TiO_2 (10 mM) plus NaBr (10 mM) was irradiated with fluences as high as 120 J/cm^2 of UVA (2 hours) with stirring. The mixture was centrifuged and the UV-vis absorption spectrum measured. There was no detectable peak at 267 nm (Br_3^- has a molar absorption coefficient of 40,900 at 267 nm) [25]. Moreover we used HPLC to try to identify Br_3^- as described by Weinberg and Yamada [25]. These authors used an anion exchange column (AS12) eluted by a carbonate/bicarbonate gradient, but we were unable to detect any peak corresponding to tribromide, while we were able to detect tribromide produced by the positive control reaction of bromine and bromide.

Bacterial strains and culture conditions

We used a methicillin-resistant *Staphylococcus aureus* (MRSA), CA-MRSA strain USA300 LAC (Los Angeles County clone), *Escherichia coli* K12 (ATCC, Manassass VA) and *Candida albicans* DAY286 reference strain (a gift from Aaron Mitchell, Department of Microbiology, Columbia University, New York, NY). Bacterial cells were grown in brain-heart infusion (BHI) medium at 37°C and *Candida* cells were grown in yeast extract peptone dextrose (YPD) media at 30°C . Cells were grown overnight to stationary phase and

refreshed for 2 hours for bacteria and 4 hours for *Candida* the next day to mid-log phase. Cells were collected by centrifugation at 3500 rpm for 10 minutes and resuspended in phosphate buffer at a density of 10^8 cells/mL for bacteria and 10^7 cells/mL for *Candida* for further experiments. Cell numbers were estimated by measuring the optical density [OD] at 600 nm (OD of 0.5= 10^8 cells/mL). To enumerate CFU/mL a 10 μ L aliquot of cells was serially diluted 10-fold in PBS to give dilutions of 10^{-1} to 10^{-5} times in addition to the original concentration, and 10 μ L aliquots of each dilution were streaked horizontally on square BHI (bacteria) or YPD (*Candida*) agar plates. Plates were streaked in triplicate and incubated for 18 hours at 30°C (*Candida*) or 37°C in the dark to allow colony formation.

Antimicrobial photocatalysis

A cell suspension consisting of 10^8 cells/mL for bacteria or 10^7 cells/mL for *Candida* was mixed with 10mM TiO₂ in the presence of various different concentrations of NaBr. Then 500 μ L of this mixture was transferred to a 24-well plate and illuminated at room temperature using UVA light under magnetic stirring. The irradiance was fixed at 16 mW/cm² (1 J/cm² delivered in 1 min). No elevation in temperature (< 1°C) was found. Cells in control group were incubated in the dark for the same time as the treatment groups (30 minutes). After each dose of UVA light had been delivered 10 μ L aliquots were withdrawn and serially diluted and streaked on BHI agar plates according to the method of Jett et al [26]. CFU were counted after overnight incubation at 37°C or 30°C for *Candida*.

Addition of bacteria after light activation of TiO₂/NaBr

To investigate the killing effect of the solution produced after light activation, we added aliquots of illuminated TiO₂/NaBr solution to the bacterial cells. The bacterial pellet was collected by centrifuging 400 μ L of 10^8 cells/mL MRSA or *E.coli* cells in BHI at 4000rpm for 5mins. 500 μ L of 10mM TiO₂ with addition of 10mM NaBr was illuminated with different doses of UVA light with stirring. At the completion of each illumination, aliquots (400 μ L) of the suspension were added to the bacterial pellet and gently resuspended. After 30 minutes incubation time, 10 μ L aliquots were taken from each group to determine colony-forming units (CFU).

Myeloperoxidase (MPO/H₂O₂) Antimicrobial Studies

A stock solution (0.25U/mL) of MPO was prepared by adding 5U of MPO in 10mL 50/50 glycerol/H₂O and kept at -20°C. Suspensions of bacteria (10^8 CFU/mL) were incubated at room temperature with MPO 10 mU/mL and H₂O₂ 100 μ M with and without added NaBr (ranging from 10 nM to 100 mM) in either 50 mM phosphate buffer pH 5.5 or pH 7.4 for 60 minutes (final volume 1 mL). At the completion of the incubation, aliquots, (100 μ L) were taken from each tube to determine CFU as described above.

Statistics

Data are presented as mean \pm SD. We used one-way ANOVA for comparisons and the Tukey post-hoc test was used for pairwise comparisons. Significance was defined as p<0.05. SPSS statistics V17.0 (IBM, Armonk, NY) was used for analysis.

Results

Addition of sodium bromide potentiates TiO₂ antimicrobial photocatalysis

When MRSA cells (10(8) CFU/mL; Gram-positive bacteria) were irradiated with UVA light in the presence of TiO₂ (10 mM) there was a light dose-dependent loss of viability reaching almost 2 logs of killing at 30 J/cm². However when 10 mM NaBr was added to the mixture the antimicrobial effect was potentiated by 1–3 logs of extra killing (Figure 1A). When the experiment was repeated with *E. coli* (10(8) CFU/mL; Gram-negative bacteria) there was a light dose-dependent killing, with TiO₂ and UVA light alone giving over 4 logs of killing at 30 J/cm². However when 10 mM NaBr was added, there was an extra 1–3 logs of bacterial killing on top of that seen with photocatalysis alone (Figure 1B). When the experiment was repeated with 10(7) CFU/mL of *C. albicans* (fungal yeast) we found similar results. With TiO₂ and UVA light alone there was up to 4 logs of killing, but this was increased by 1–2 logs of additional killing by the addition of 10 mM NaBr to the mixture.

Because of comparisons with the antimicrobial effects of the myeloperoxidase + H₂O₂ + bromide system (see later) we investigated the effects of reducing the pH to 5.5 on the efficiency of the antimicrobial photocatalysis. There were no significant differences between the killing of MRSA and *E. coli* with UVA irradiated TiO₂ (with and without NaBr) when carried out in phosphate buffer at pH 7.4 and at pH 5.5 (data not shown)

Bromide concentration response

In order to find the most effective concentration of bromide for potentiating the killing we carried out an experiment where we used a series of light doses delivered to bacteria stirred with TiO₂ (10 mM) and increasing concentrations of bromide. Figure 2A shows that for MRSA 1.5 mM bromide was sufficient to give 2–3 logs of extra killing, while for *E. coli* 10 mM bromide gave an impressive 4 logs of extra killing (Figure 2B), and for *C. albicans* 10 mM bromide also gave 4 logs of extra killing (Figure 2C),

Killing after light

We wished to investigate how much of the synergistic killing was due to production of a relatively long-lived stable antimicrobial species, so we added microbial cells at different times after completion of light delivery. Figure 3A shows that when MRSA cells were added to a suspension of TiO₂ that had been treated with 40 J/cm² of UVA light in the presence of 10 mM or 100 mM bromide there was about 1.5 logs of killing, but no killing at all without bromide. When the bacteria were added to the irradiated suspension 30 min after the end of the illumination period there was the same degree of killing, but when 2 hours was allowed to elapse after the light there was no killing at all. Very similar results were obtained when the experiment was repeated with *E. coli* (Figure 3B).

Chemical assays

In order to gain some information on the identity of the long-lived antimicrobial chemical species that was produced in an irradiated suspension of TiO₂ and bromide, we added 3,3', 5,5'-tetramethylbenzidine (TMB) to the suspension after the end of the illumination. TMB is a widely used chromogenic substrate for detecting oxidizing species, which is oxidized by

hypobromite and hypoiodite [27]. Figure 4A shows that when 10 mM bromide was added to irradiated TiO₂ there was a light dose-dependent increase in oxidized TMB with as little as 5J/cm² not seen in the absence of bromide. As we wished to determine how stable this TMB-oxidizing species was (considering the loss of the antimicrobial activity over 2 hours) we added TMB at different times after the end of the illumination period. Figure 4B shows that after 5 min over 50% of the TMB oxidizing species had decayed, with over 80% gone after 30 min and 100% gone after 2 hours.

We carried out bromination of N-acetyl tyrosine ethyl ester to provide chemical proof of the formation of a reactive bromine species that was produced in the presence of TiO₂, NaBr, and UVA. By analogy with studies that have been carried out to demonstrate nitration of tyrosine derivatives [28], we employed N-acetyl tyrosine ethyl ester as the substrate for the reaction, and this substrate was brominated to produce the product N-acetyl-3-bromotyrosine ethyl ester. We used LC-MS to identify the product (C₁₃H₁₅NBrO₄⁻ m/z = 328.02 and 330.02) and were able to construct a linear light-dose response curve shown in Figure 5.

In principle the long-lived antimicrobial reactive species could have been bromine or hypobromite or a mixture of both. In order to try and distinguish between hypobromite and bromine (which would be present as tribromide anion in the presence of a high concentration of bromide) we used spectrophotometry at 267 nm (Br₃⁻ has a molar absorption coefficient of 40,900 at 267 nm) [25] and HPLC using an anion exchange column [25]. Despite numerous attempts we were unable to detect any formation of tribromide by spectrophotometry or by HPLC.

ROS-specific fluorescence probes

In order to gain some information on whether a specific reactive oxygen species (ROS) produced by the illuminated TiO₂ was responsible for oxidizing the bromide, we used two fluorescence probes for specific ROS that we had previously used in photodynamic therapy studies [29, 30] and asked whether their activation would be quenched by addition of bromide. SOSG is relatively specific for singlet oxygen and HPF is relatively specific for detecting hydroxyl radicals. Figure 6A shows that there was modest but significant quenching of light-activated SOSG fluorescence by addition of 10 mM bromide. Figure 6B shows that in contrast there was no significant quenching of the photoactivation of the HPF probe.

Comparison with myeloperoxidase/H₂O₂/bromide system

The closest comparison to bromide potentiation of TiO₂ antimicrobial photocatalysis, appeared to be the antimicrobial peroxidase/H₂O₂/bromide system [31]. Although several different peroxidase enzymes will mediate this antimicrobial system (some with different specificities for bromide compared to chloride and iodide), we chose to test myeloperoxidase (MPO) as this has been widely studied. The antimicrobial effects of the MPO/H₂O₂/Br⁻ system have been reported to be sensitive to pH, so we tested it in phosphate buffer at pH 7.4 and at pH 5.5. Figure 7A shows the killing of MRSA incubated with 10 mU of MPO and 100 μM H₂O₂ for one hour in the presence of a wide range of

bromide concentrations ranging from 10 nM to 100 mM (8 orders of magnitude) in the 2 different pH buffers. It can be seen that the killing was dramatically better at pH 5.5 where as low a bromide concentration as 100 nM showed some bacterial killing, while at pH 7.4 it was necessary to increase the bromide concentration to 10 mM to get any killing. Figure 7B shows the situation was even more pronounced with *E. coli* with killing at pH 5.5 starting at 100 nM bromide and with eradication (zero CFU remaining) at 100 μ M, while 10 mM bromide was needed for killing at pH 7.4.

Discussion

We have shown for the first time, that addition of the simple non-toxic inorganic salt, sodium bromide to the antimicrobial TiO₂ photocatalysis system potentiates killing of a broad-spectrum of microorganisms by up to 3 logs. The mechanism appears to be based on a 2-electron oxidation of bromide to hypobromite. The order of susceptibility of the different classes of microbial cells was somewhat surprising. We found that Gram-negative *E. coli* was most susceptible, *C. albicans* was intermediate, and Gram-positive MRSA was least susceptible. It is well known in the field of antimicrobial photodynamic inactivation (aPDI) that Gram-positive bacteria are most susceptible, fungal yeasts such as *C. albicans* are intermediate, while Gram-negative bacteria are least susceptible [32]. The pronounced susceptibility difference in the case of aPDI is attributed to differences in permeability of the cell wall, that restricts penetration of the photosensitizer into sensitive parts of the cell especially in Gram-negative bacteria [33, 34].

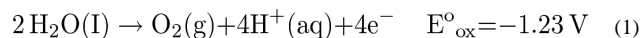
Many other laboratories have investigated in detail many innovative approaches to improving antimicrobial TiO₂ photocatalysis. Many of these approaches have been directed towards shifting the wavelength of the activating light away from the UVA range required by P25, and towards the visible range (blue, green, red, or even NIR). There have been a wide range of “doping” procedures using various impurities reported [35] with elements such as nitrogen [36], platinum [19], molybdenum [37], iron and aluminum [38], various organic compounds [17] etc.

We demonstrated the existence of a reactive brominating species, by brominating the tyrosine derivative, N-acetyl tyrosine ethyl ester, to form the product, N-acetyl 3-bromotyrosine ethyl ester, detected by LC-MS. This method was chosen as a similar reaction scheme had been used to detect the nitration of tyrosine produced by a photocontrollable peroxyxynitrite generator based on N-methyl-N-nitrosoaminophenol [28].

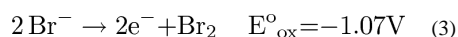
To study the mechanism we first asked whether the oxidation of bromide could be caused by one of the reactive oxygen species formed during TiO₂ photocatalysis, namely hydroxyl radicals or singlet oxygen [17]. We used the fluorescent ROS probes HPF (detects HO•) and SOSG (detects ¹O₂). The data (Figure 5) showed no quenching of HPF and only minor quenching of SOSG. Although hydroxyl radical has a redox potential (+ 2.31V) that is more than enough to oxidize bromide (−0.78V), singlet oxygen does not (+ 0.64V) [18]. The minor inhibition of the TiO₂-mediated photoactivation of SOSG by bromide is probably caused by the physical quenching of ¹O₂ caused by its collision with bromide ions in a similar manner to that shown for iodide ions [39]. Therefore we assumed that bromide

oxidation was caused by a direct oxidation arising from the photoactivated TiO₂ rather than oxidation by an intermediate oxygen-containing oxidizing species.

When TiO₂ is irradiated by UVA light it acts as an oxidizing agent, due to the positive holes generated in the valence band by excitation of electrons into the valence band. Water can be oxidized to oxygen



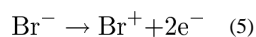
showing that the oxidizing potential is at least +1.23V. The redox potential of bromide to hypobromite is lower (-0.76V) than the redox potential for bromide to bromine (-1.07V) showing that bromide may be preferentially oxidized to hypobromite rather than bromine.



However there is another difference. The oxidation to hypobromite is a true 2-electron oxidation, while the oxidation to bromine is two separate 1-electron oxidations that proceed via the short-lived intermediate bromine radical



By contrast the first step in the 2-electron oxidation to hypobromite is



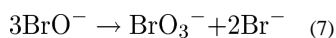
Bromide initially reacts to form the bromonium cation that subsequently reacts with water to form hypobromite



The additional microbial killing in our studies could not be completely explained by generation of hypobromite. Only about 1 log of killing could be obtained when the microbial cells were added immediately after the light (see Figure 3) while up to 3 additional logs of killing could be obtained when the microbial cells were present during the illumination. The additional killing could be attributed to a short-lived reactive intermediate formed during the photoexcitation. The proposed intermediate in the oxidation of bromide to hypobromite, is bromonium cation, which is a highly reactive brominating electrophile [40] and may be responsible for the short-lived antimicrobial species that is only present during the illumination period.

It is not immediately apparent why photoactivated TiO₂ should preferentially carry out 2-electron oxidations rather than 1-electron oxidations. In reality it may be the case that the lower redox potential of the hypobromite reaction is the principal determining factor

Hypobromite is an unstable species and disproportionates to form bromate and bromide



This reaction is probably responsible for the observed time-dependent loss of the antimicrobial activity of the irradiated TiO₂ suspension containing added bromide.

There has been a report of the use organic molecules to study the interaction of photoactivated TiO₂ with bromide anion [41]. Using cyclohexene as a probe they proposed a mechanism in which the photoexcited TiO₂ carried out a one-electron oxidation of adsorbed bromide, producing surface-bound bromine atoms. These potentially could abstract hydrogen from cyclohexene to initiate autoxidation or could migrate along the semiconductor surface, producing bromine. The difference in the results could be explained by the fact that their experiments were conducted in an organic solvent (anhydrous acetonitrile) while we used water. Another study looked at the effect of chloride on TiO₂ photocatalysis (measuring dye decolorization) [42]. They found that in aqueous solution a low concentration of Cl⁻ (< 0.01 M) showed little influence but a high concentration of Cl⁻ (> 0.1 M) had a very different influence on the decolorization of dyes: a significant inhibition for methylene blue but a great promotion for orange II.

Peroxidases are a class of enzyme that use a peroxide (most often hydrogen peroxide) to oxidize an organic or inorganic substrate. Many peroxidase enzymes (including a class known as “haloperoxidases”) oxidize a halide ion to the respective hypohalite ion. Heme peroxidases operate by a well-established mechanism involving an intermediate (called “compound I”) (formed by a 2-electron oxidation) that has oxygen attached to the heme-iron (Fe(IV) and a radical cation present on the porphyrin ring [43]. Myeloperoxidase, which occurs in the granules of neutrophils [44], is a good example of a peroxidase with a pronounced antimicrobial activity. MPO can oxidize chloride to hypochlorite and this species is believed to be a major weapon in the arsenal of neutrophils to kill bacteria and other pathogenic microorganisms [45]. MPO plus hydrogen peroxide also forms hypoiodite from iodide and hypobromite from bromide [31]. In agreement with previous studies using MPO/H₂O₂/I⁻ [46], we found that the antimicrobial activity of MPO/H₂O₂/Br⁻ system was strongly dependent on the pH. The antibacterial activity against bacteria (and especially the Gram-negative *E. coli*) was several orders of magnitude more pronounced at pH 5.5 compared to pH 7.4. We have been unable to find a convincing explanation of this pronounced difference between pH values. Interestingly we did not find a difference between the antimicrobial activity of the TiO₂/UVA/Br⁻ system at pH 5.5 and 7.4. Moreover at pH 5.5 the MPO/H₂O₂/Br⁻ system was active with bromide concentrations that were very low in comparison with the TiO₂/UVA/Br⁻ system.

A recent publication suggested that hypobromite was the “most powerful endogenous electrophile” [47]. Although hypobromite is a less powerful oxidizing agent than

hypochlorite, it is a more powerful halogenating agent. It is at present uncertain how much of the microbicidal effects of hypochlorites are due to their oxidizing ability and how much is due to their halogenating ability. There is an enzyme that is widely distributed in marine life-forms called vanadium bromoperoxidase (non heme-containing) whose purpose is to introduce bromine atoms into a variety of brominated secondary metabolites that are common in marine organisms [40]. It is at present uncertain how effective vanadium bromoperoxidase/H₂O₂/Br⁻ would be in killing microorganisms.

It is at present uncertain whether our discovery will have any practical applications in the real world. The requirement for millimolar concentrations of bromide for significant potentiation of the antimicrobial activity may prove a limiting factor. Could TiO₂ be doped with an immobilized form of bromide anion to form an improved photoactivated antimicrobial surface? If so would it still be effective? Are there any situations when it would be realistic to add a solution of bromide to an aqueous solution that was required to be photodisinfected? Clearly further research would be needed to answer these provocative questions.

Supplementary Material

Refer to Web version on PubMed Central for supplementary material.

Acknowledgments

This work was supported by US NIH grant R01 AI050875. Yu Kushida was supported by the Research Experience for Undergraduates (REU) Program of the National Science Foundation under Award Number EEC-1358296. We are grateful to Dr Brijesh Bhayana for help with analytical chemistry.

References

1. Li Puma G, Rodriguez-Gonzalez V, Perez-Larios A. Photocatalysis: from the treatment of emerging contaminants to energy conversion. *J Hazard Mater.* 2013; 263(Pt 1):1. [PubMed: 24267571]
2. Oliveira HG, Ferreira LH, Bertazzoli R, Longo C. Remediation of 17-alpha-ethinylestradiol aqueous solution by photocatalysis and electrochemically-assisted photocatalysis using TiO₂ and TiO₂/WO₃ electrodes irradiated by a solar simulator. *Water Res.* 2015; 72:305–314. [PubMed: 25238917]
3. Saggiaro EM, Oliveira AS, Pavesi T, Maia CG, Ferreira LF, Moreira JC. Use of titanium dioxide photocatalysis on the remediation of model textile wastewaters containing azo dyes. *Molecules.* 2011; 16:10370–10386. [PubMed: 22169940]
4. Byrne JA, Dunlop PS, Hamilton JW, Fernandez-Ibanez P, Polo-Lopez I, Sharma PK, Vennard AS. A review of heterogeneous photocatalysis for water and surface disinfection. *Molecules.* 2015; 20:5574–5615. [PubMed: 25830789]
5. Kim S, Ghafoor K, Lee J, Feng M, Hong J, Lee DU, Park J. Bacterial inactivation in water, DNA strand breaking, and membrane damage induced by ultraviolet-assisted titanium dioxide photocatalysis. *Water Res.* 2013; 47:4403–4411. [PubMed: 23764591]
6. Rizzo L, Della Sala A, Fiorentino A, Li Puma G. Disinfection of urban wastewater by solar driven and UV lamp - TiO₂ photocatalysis: effect on a multi drug resistant *Escherichia coli* strain. *Water Res.* 2014; 53:145–152. [PubMed: 24525064]
7. Robertson PK, Robertson JM, Bahnemann DW. Removal of microorganisms and their chemical metabolites from water using semiconductor photocatalysis. *J Hazard Mater.* 2012; 211–212:161–171.

8. Yamada N, Suzumura M, Koiwa F, Negishi N. Differences in elimination efficiencies of *Escherichia coli* in freshwater and seawater as a result of TiO₂ photocatalysis. *Water Res.* 2013; 47:2770–2776. [PubMed: 23523173]
9. Vidal A. Developments in solar photocatalysis for water purification. *Chemosphere.* 1998; 36:2593–2606. [PubMed: 9570109]
10. Lilja M, Forsgren J, Welch K, Astrand M, Engqvist H, Stromme M. Photocatalytic and antimicrobial properties of surgical implant coatings of titanium dioxide deposited through cathodic arc evaporation. *Biotechnol Lett.* 2012; 34:2299–2305. [PubMed: 22941372]
11. Suketa N, Sawase T, Kitaura H, Naito M, Baba K, Nakayama K, Wennerberg A, Atsuta M. An antibacterial surface on dental implants, based on the photocatalytic bactericidal effect. *Clin Implant Dent Relat Res.* 2005; 7:105–111. [PubMed: 15996357]
12. Nakamura H, Tanaka M, Shinohara S, Gotoh M, Karube I. Development of a self-sterilizing lancet coated with a titanium dioxide photocatalytic nano-layer for self-monitoring of blood glucose. *Biosens Bioelectron.* 2007; 22:1920–1925. [PubMed: 16987650]
13. Yin ZF, Wu L, Yang HG, Su YH. Recent progress in biomedical applications of titanium dioxide. *Phys Chem Chem Phys.* 2013; 15:4844–4858. [PubMed: 23450160]
14. Brown EM, Allen LL, Pyles H, Solis J, Wileman TA, Willadsen GB. Advancements in using TiO₂ bionanoconjugates for precision degradation of intracellular biological structures. *J Biomed Nanotechnol.* 2013; 9:539–550. [PubMed: 23621012]
15. Foster HA, Ditta IB, Varghese S, Steele A. Photocatalytic disinfection using titanium dioxide: spectrum and mechanism of antimicrobial activity. *Appl Microbiol Biotechnol.* 2011; 90:1847–1868. [PubMed: 21523480]
16. Wang H, Li J, Quan X, Wu Y, Li G, Wang F. Formation of hydrogen peroxide and degradation of phenol in synergistic system of pulsed corona discharge combined with TiO₂ photocatalysis. *J Hazard Mater.* 2007; 141:336–343. [PubMed: 16920259]
17. Buchalska M, Labuz P, Bujak L, Szewczyk G, Sarna T, Mackowski S, Macyk W. New insight into singlet oxygen generation at surface modified nanocrystalline TiO₂--the effect of near-infrared irradiation. *Dalton Trans.* 2013; 42:9468–9475. [PubMed: 23665700]
18. Vatansever F, de Melo WC, Avci P, Vecchio D, Sadasivam M, Gupta A, Chandran R, Karimi M, Parizotto NA, Yin R, Tegos GP, Hamblin MR. Antimicrobial strategies centered around reactive oxygen species - bactericidal antibiotics, photodynamic therapy and beyond. *FEMS Microbiol Rev.* 2013
19. Mitoraj D, Janczyk A, Strus M, Kisch H, Stochel G, Heczko PB, Macyk W. Visible light inactivation of bacteria and fungi by modified titanium dioxide. *Photochem Photobiol Sci.* 2007; 6:642–648. [PubMed: 17549266]
20. Wong CL, Tan YN, Mohamed AR. A review on the formation of titania nanotube photocatalysts by hydrothermal treatment. *J Environ Manage.* 2011; 92:1669–1680. [PubMed: 21450395]
21. Ohtani B, Prieto-Mahaney OO, Li D, Abe R. What is Degussa (Evonik) P25? Crystalline composition analysis, reconstruction from isolated pure particles and photocatalytic activity test. *J Photochem Photobiol A : Chemistry.* 2010; 216:179–182.
22. Vecchio D, Gupta A, Huang L, Landi G, Avci P, Rodas A, Hamblin MR. Bacterial photodynamic inactivation mediated by methylene blue and red light is enhanced by synergistic effect of potassium iodide. *Antimicrob Agents Chemother.* 2015
23. Yin R, Wang M, Huang YY, Landi G, Vecchio D, Chiang LY, Hamblin MR. Antimicrobial photodynamic inactivation with decacationic functionalized fullerenes: oxygen independent photokilling in presence of azide and new mechanistic insights. *Free radical biology & medicine.* 2015; 79:14–27. [PubMed: 25451642]
24. Zhang Y, Dai T, Wang M, Vecchio D, Chiang LY, Hamblin MR. Potentiation of antimicrobial photodynamic inactivation mediated by a cationic fullerene by added iodide: in vitro and in vivo studies. *Nanomedicine.* 2015; 10:603–614. [PubMed: 25723093]
25. Weinberg HS, Yamada H. Post-ion-chromatography derivatization for the determination of oxyhalides at sub-PPB levels in drinking water. *Anal Chem.* 1998; 70:1–6. [PubMed: 9435465]
26. Jett BD, Hatter KL, Huycke MM, Gilmore MS. Simplified agar plate method for quantifying viable bacteria. *Biotechniques.* 1997; 23:648–650. [PubMed: 9343684]

27. Li H, Cao Z, Zhang G, Thannickal VJ, Cheng G. Vascular peroxidase 1 catalyzes the formation of hypohalous acids: characterization of its substrate specificity and enzymatic properties. *Free radical biology & medicine*. 2012; 53:1954–1959. [PubMed: 22982576]
28. Ieda N, Nakagawa H, Peng T, Yang D, Suzuki T, Miyata N. Photocontrollable peroxy nitrite generator based on N-methyl-N-nitrosoaminophenol for cellular application. *J Am Chem Soc*. 2012; 134:2563–2568. [PubMed: 22239467]
29. Huang L, St Denis TG, Xuan Y, Huang YY, Tanaka M, Zadlo A, Sarna T, Hamblin MR. Paradoxical potentiation of methylene blue-mediated antimicrobial photodynamic inactivation by sodium azide: role of ambient oxygen and azide radicals. *Free Radic Biol Med*. 2012; 53:2062–2071. [PubMed: 23044264]
30. Huang L, Xuan Y, Koide Y, Zhiyentayev T, Tanaka M, Hamblin MR. Type I and Type II mechanisms of antimicrobial photodynamic therapy: An in vitro study on gram-negative and gram-positive bacteria. *Lasers Surg Med*. 2012; 44:490–499. [PubMed: 22760848]
31. Klebanoff SJ. Myeloperoxidase-halide-hydrogen peroxide antibacterial system. *J Bacteriol*. 1968; 95:2131–2138. [PubMed: 4970226]
32. Hamblin MR, Hasan T. Photodynamic therapy: a new antimicrobial approach to infectious disease? *Photochem Photobiol Sci*. 2004; 3:436–450. [PubMed: 15122361]
33. Merchat M, Spikes JD, Bertoloni G, Jori G. Studies on the mechanism of bacteria photosensitization by meso-substituted cationic porphyrins. *J Photochem Photobiol B*. 1996; 35:149–157. [PubMed: 8933721]
34. Minnock A, Vernon DI, Schofield J, Griffiths J, Parish JH, Brown SB. Mechanism of uptake of a cationic water-soluble pyridinium zinc phthalocyanine across the outer membrane of *Escherichia coli*. *Antimicrob Agents Chemother*. 2000; 44:522–527. [PubMed: 10681312]
35. Liou JW, Chang HH. Bactericidal effects and mechanisms of visible light-responsive titanium dioxide photocatalysts on pathogenic bacteria. *Arch Immunol Ther Exp (Warsz)*. 2012; 60:267–275. [PubMed: 22678625]
36. Yu B, Lau WM, Yang J. Preparation and characterization of N-TiO₂ photocatalyst with high crystallinity and enhanced photocatalytic inactivation of bacteria. *Nanotechnology*. 2013; 24:335705. [PubMed: 23892455]
37. Fisher L, Ostovapour S, Kelly P, Whitehead KA, Cooke K, Storgards E, Verran J. Molybdenum doped titanium dioxide photocatalytic coatings for use as hygienic surfaces: the effect of soiling on antimicrobial activity. *Biofouling*. 2014; 30:911–919. [PubMed: 25184432]
38. Schlur L, Begin-Colin S, Gilliot P, Gallart M, Carre G, Zafeiratos S, Keller N, Keller V, Andre P, Greneche JM, Hezard B, Desmots MH, Pourroy G. Effect of ball-milling and Fe-/Al-doping on the structural aspect and visible light photocatalytic activity of TiO₂ towards *Escherichia coli* bacteria abatement. *Mater Sci Eng C Mater Biol Appl*. 2014; 38:11–19. [PubMed: 24656347]
39. Rosenthal I, Frimer A. The quenching effect of iodide ion on singlet oxygen. *Photochem Photobiol*. 1976; 23:209–211. [PubMed: 1265147]
40. Butler A, Carter-Franklin JN. The role of vanadium bromoperoxidase in the biosynthesis of halogenated marine natural products. *Nat Prod Rep*. 2004; 21:180–188. [PubMed: 15039842]
41. Fox MA, Pettit TL. Use of Organic Molecules as Mechanistic Probes for Semiconductor-Mediated Photoelectrochemical Oxidations: Bromide Oxidation. *J Org Chem*. 1885; 50:5013–5015.
42. Yang SY, Chen YX, Lou LP, Wu XN. Involvement of chloride anion in photocatalytic process. *J Environ Sci (China)*. 2005; 17:761–765. [PubMed: 16312998]
43. Hiner AN, Raven EL, Thorneley RN, Garcia-Canovas F, Rodriguez-Lopez JN. Mechanisms of compound I formation in heme peroxidases. *J Inorg Biochem*. 2002; 91:27–34. [PubMed: 12121759]
44. Klebanoff SJ, Kettle AJ, Rosen H, Winterbourn CC, Nauseef WM. Myeloperoxidase: a front-line defender against phagocytosed microorganisms. *J Leukoc Biol*. 2013; 93:185–198. [PubMed: 23066164]
45. Nauseef WM. Myeloperoxidase in human neutrophil host defence. *Cell Microbiol*. 2014; 16:1146–1155. [PubMed: 24844117]
46. Klebanoff SJ. The iron-H₂O₂-iodide cytotoxic system. *J Exp Med*. 1982; 156:1262–1267. [PubMed: 6296262]

47. Ximenes VF, Morgon NH, de Souza AR. Hypobromous acid, a powerful endogenous electrophile: Experimental and theoretical studies. *J Inorg Biochem.* 2015; 146:61–68. [PubMed: 25771434]

Author Manuscript

Author Manuscript

Author Manuscript

Author Manuscript

Highlights

Antimicrobial killing mediated by photocatalysis using titanium dioxide and UVA light is potentiated by addition of sodium bromide.

Broad-spectrum effect active against Gram-positive and Gram-negative bacteria and fungi.

Mechanism involves oxidation of bromide to produce a brominating agent likely to be hypobromite.

Has elements in common with the antimicrobial system (myeloperoxidase + hydrogen peroxide + bromide)

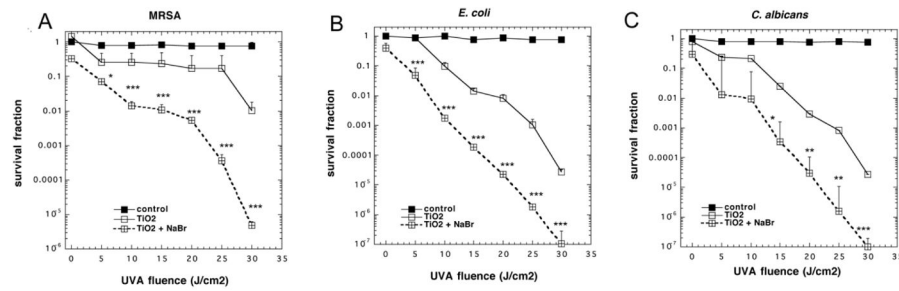


Figure 1. Antimicrobial TiO₂ photocatalysis of microbial cells is potentiated by addition of NaBr Cells were stirred in the presence of TiO₂ (0 or 10 mM) and NaBr (0 or 10 mM) while being exposed to increasing fluences of UVA light. (A) MRSA (10⁸) cells/mL; (B) *E. coli* (10⁸) cells/mL; (C) *C. albicans* (10⁷) cells/mL). Values are means of 3 repetitions and bars are SD. * p < 0.05; ** p < 0.01; *** p < 0.001 for TiO₂ + NaBr vs TiO₂ alone.

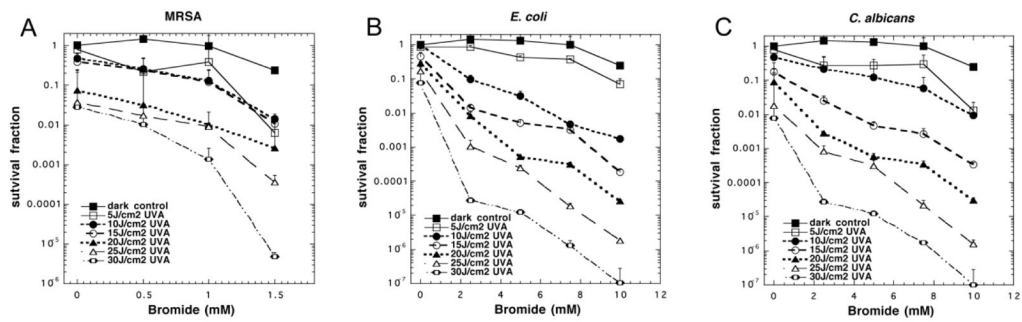


Figure 2. Effect of bromide concentration on antimicrobial TiO₂ photocatalysis

Cells were stirred in the presence of 10 mM TiO₂ with addition of a range of concentrations of NaBr while being exposed to increasing fluences of UVA light. (A) MRSA (0–1.5 mM NaBr); (B) *E. coli* (0–10 mM NaBr); (C) *C. albicans* (0–10 mM NaBr). Values are means of 3 repetitions and bars are SD.

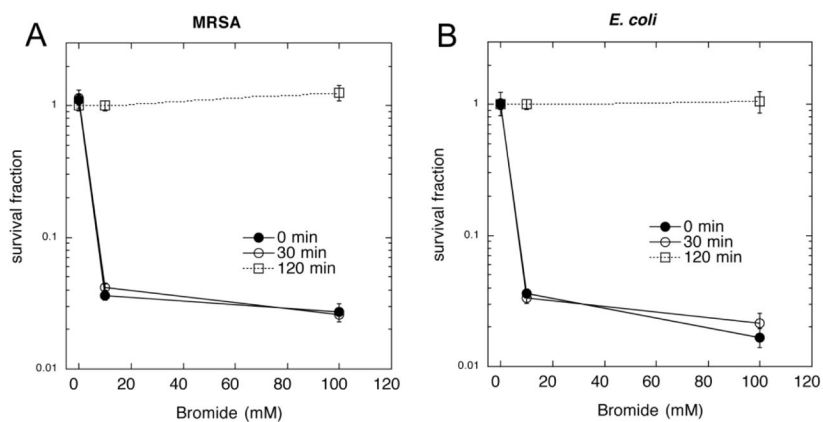


Figure 3. Killing of bacteria added to photoactivated TiO₂ after light

TiO₂ (10 mM) was stirred with NaBr (0, 10, or 100 mM) under UVA light (40 J/cm²).

MRSA (A) or *E. coli* (B) cells (10(8) cells/mL) were then added at 0, 30 or 120 minutes after the end of the illumination and incubated for 1 hour. Values are means of 3 repetitions and bars are SD.

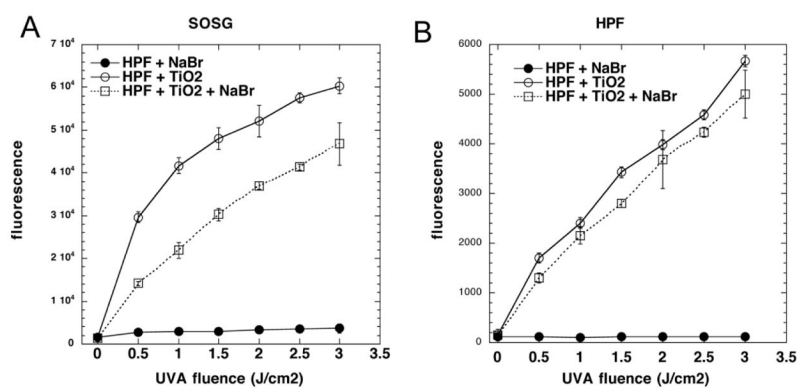


Figure 4. Oxidation of TMB by photoactivated TiO₂ after light

(A) TiO₂ (10 mM) was stirred with NaBr (0 or 10 mM) under UVA light (1–5 J/cm²). A solution of TMB (0.1 mg/mL) was then added and incubated for 3 hours. (B) TiO₂ (10 mM) was stirred with NaBr (10 mM) under UVA light (0–5 J/cm²). At different times after the end of the illumination, 50 μ l aliquots of the mixture was added to 1 mL TMB (0.1 mg/mL). Values are means of 6 wells and bars are SD.

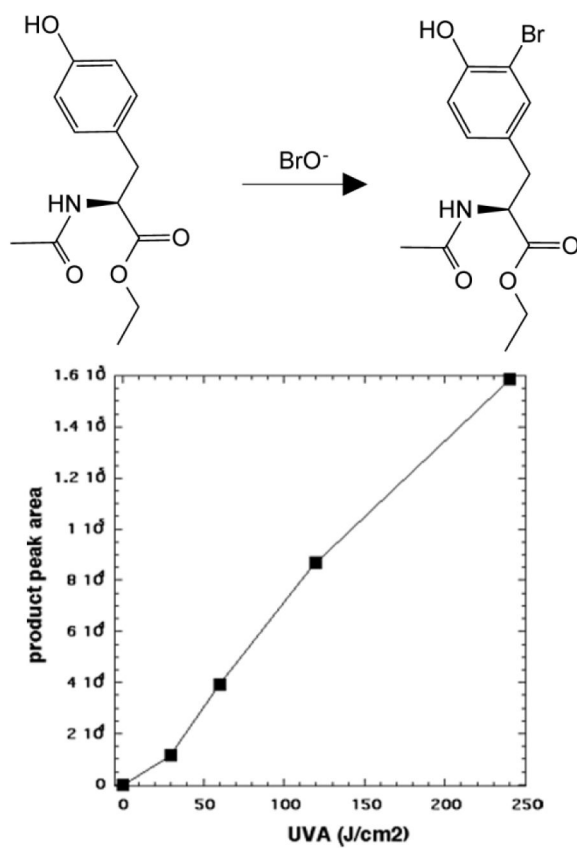


Figure 5. Light-dose dependent bromination of N-acetyl tyrosine ethyl ester by TiO_2 + NaBr irradiated with UVA

3-bromo N-acetyltyrosine ethyl ester was quantified after increasing fluences of UVA light had been delivered to a mixture of TiO_2 , NaBr and N-acetyltyrosine ethyl ester using LC-MS.

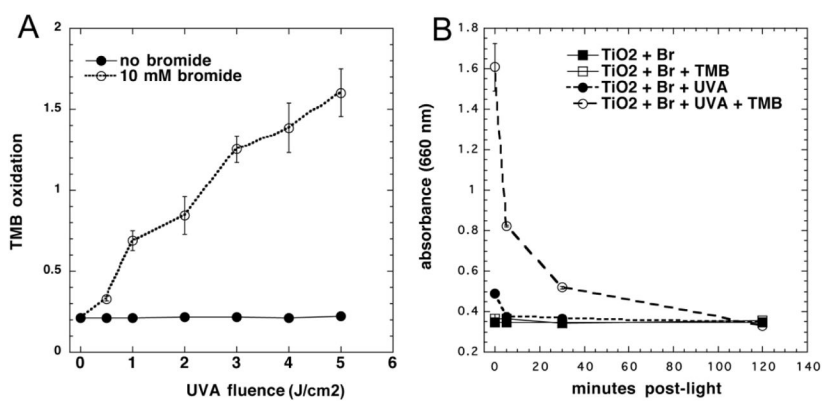


Figure 6. Activation of ROS-specific fluorescence probes by photoactivated TiO₂ Probe was illuminated with UVA light (TiO₂ (10 mM) was illuminated with UVA light (0–3 J/cm²) in the presence of NaBr (10 mM), TiO₂ (10 mM) or both (10 mM NaBr + 10 mM TiO₂). Fluorescence was measured in plate reader after each aliquot of light. (A) SOSG; (B) HPF. Values are means of 6 wells and bars are SD.

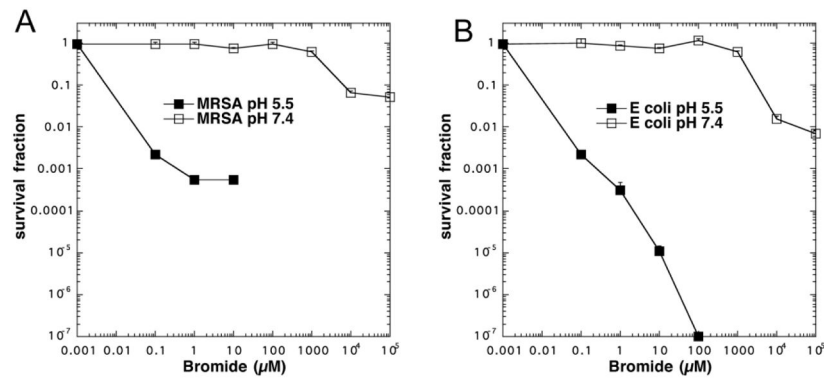


Figure 7. Antimicrobial effects of MPO/H₂O₂/bromide system

Bacteria (10⁸ cells/mL) were incubated for 1 hour with MPO (10 mU), H₂O₂ (100 μM) and a large range of bromide concentrations (10 nM to 100 mM) in two different 50 mM phosphate buffers (pH 5.5 and pH 7.4). (A) MRSA; (B) *E. coli*. Values are means of 3 repetitions and bars are SD.